Monitoring damage evolution in a tectonically faulted clay shale — an experiment of the Mont Terri URL

Martin Ziegler
Swiss Federal Office of Topography (swisstopo), St. Ursanne, Switzerland

Markus Furche, Thies Beilecke, Thomas Burschil
German Federal Institute for Geosciences and Natural Resources (BGR), Hannover, Germany

Anne Obermann
Swiss Seismological Service (SED), ETH Zurich, Zurich, Switzerland

Qinghua Lei, Chenxi Zhao, Simon Loew
Department of Earth Sciences, ETH Zurich, Zurich, Switzerland

ABSTRACT: The Progressive Failure (PF) project explores experimentally and numerically structurally-controlled damage evolution in faulted Opalinus Clay shale at 1:5 scale in the Mont Terri URL, Switzerland. The in-situ experiment consists of a central, large-diameter experiment borehole (representing a repository drift) and six monitoring boreholes. The experiment borehole intersects tectonic fault planes and a major fault zone; its air humidity is controlled to simulate open and closed drift phases. The rock mass damage evolution is recorded by manifold techniques, including borehole photogrammetry, active seismic and electrical resistivity tomographies, and recordings of pico-seismicity, aiming at detecting and observing damage initiation and evolution around the borehole. A discontinuum numerical model is built to mimic the tectonic fractures explicitly and investigate the damage evolution around the experiment borehole. This paper provides an introduction to the experiment and highlights key datasets collected over the first two years of the project.

Keywords: structurally-controlled failure, Opalinus Clay shale, in-situ experiment, electrical and seismic tomography, borehole photogrammetry, numerical discontinuum simulation.

1 INTRODUCTION

In the context of nuclear waste repositories, the integrity of the geological barrier is a major concern. In unfavourable situations, steep and acute angled fault zones may lead to deep rock mass damage and/or large caving/overbreak above repository drifts or caverns. However, the presence of tectonic fault zones with offset < 20 m at the repository depth of 800–900 m below ground surface cannot be predicted precisely nor completely from measurements (e.g., seismic investigations) carried out at the ground surface prior to repository excavation. Very critical are steeply dipping and persistent discontinuities or weak fault zones striking at angles smaller than about 30° to the tunnel axes (e.g., Bieniawski, 1989). Structurally-controlled failure may be initiated during excavation and damage the geological barrier progressively, i.e., rock damage may evolve over long periods of time, driven by hydromechanically coupled processes and delayed support reactions. Such zones can substantially reduce the effective thickness of the geological barrier and may lead to abandoning of repository drift sections for waste disposal, increasing the required subsurface space of a high-level waste (HLW)

repository. Up to now, the extent, properties, and progressive formation of such damaged zones have not been investigated under in-situ conditions. It is of central importance to evaluate fault zone hazard scenarios related to repository construction and long-term safety (Ziegler and Loew 2020).

Extensive rock mass damage and overbreak should, as much as possible, be avoided with suitable engineering measures during the construction phase. In addition, the lifetime of conventional support measures is limited and is expected to be shorter than the saturation phase of the bentonite backfill and the build-up of full swelling pressure, respectively (e.g., Birkholzer 2019 and references therein). Hence, rock mass damage may increase once the bearing capacity of support measures reduces. For deep tunnels in clay shales without effective tunnel support, large damaged zones with deep shear displacements (squeezing zones) may also form outside tectonic shear zones.

The Progressive Failure (PF) project aims at exploring structurally-controlled damage evolution in faulted Opalinus Clay shale (OPA) in a 1:5 scale in-situ experiment at the Mont Terri Underground Rock Laboratory (MT URL). Failure behaviour and damage extents of the experiment are measured with a variety of geophysical and photogrammetric tools and will be compared with numerical simulations. In this paper, we will introduce the in-situ project setup and discuss first measurement and discontinuum simulation results.

Our research addresses the following fundamental questions: (1) What is the extent and what are the detailed mechanisms of macro- and micro-scale damage in structurally-controlled overbreaks? (2) What are the fault zone properties and criteria based on which repository drift sections with faults will be excluded from nuclear waste emplacement? (3) How can and will critical faults and fault zones be detected and investigated during excavation?

2 METHODOLOGY

2.1 In-situ experiment

The PF experiment is conducted at the MT URL and consists of a 0.6 m wide and 12.9 m long, unsupported experiment borehole (BPF-7; with steel casing only in the first 2.5 m) and six monitoring boreholes of 14 m length each (BPF1–6; Figure 1a,b). The boreholes are in the Opalinus Clay shaly facies and dissect minor steeply dipping, slickensided tectonic fault planes and a major fault zone at angles ranging 20–60° (Section 3.1). For technical reasons it was not possible to carry out this experiment at smaller intersection angles. Progressive failure above the experiment borehole is monitored by tomographic methods (electrical resistivity tomography (ERT), repeated active and passive seismic measurements), and visible failures inside the experiment borehole are recorded using photogrammetry (Figure 1b,c). The details of the monitoring setups are out of the scope of this paper and given in Ziegler and Loew (2020, 2021a,b). In order to simulate the effect of ventilation and associated rock desaturation, the experiment borehole was ventilated in the first phase of the project (11/2020–07/2022) to obtain a relative humidity of about 65% inside BPF-7. In the second phase, the ventilation was stopped and we allow the rock mass to resaturate again, naturally.

2.2 Numerical simulation

To investigate the physical mechanisms that drive the emergence and evolution of macroscopic borehole overbreaks arising from microscopic damage processes, we developed a 3D numerical model based on the discrete element method. The model consists of an outer and an inner domain and includes rock anisotropy, a discrete fracture network (DFN), and the major fault zone based on borehole logging data (Figure 1d). It aims at simulating the deformation and failure behaviour of faulted OPA during the excavation phase including elastic and anelastic displacements, new fracture formation and displacement of pre-existing faults. Material properties of OPA matrix, fault planes, and fault zone are assigned to the model based on literature values to mimic the in-situ response during excavation. The implementation of the DFN and the parametrization of the mechanical model are detailed in Zhao et al. (2022).

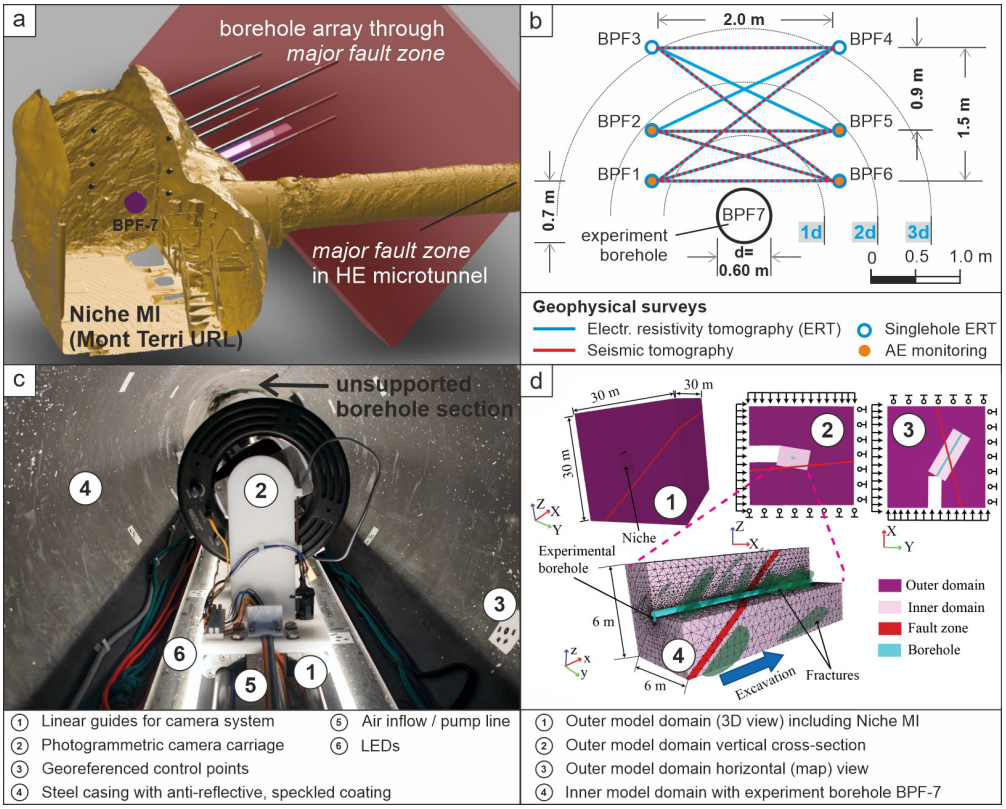

Figure 1. (a) A laser scan model (yellow; view toward SW) of the MI niche and HE microtunnel was used to estimate the intersections of a major fault zone (red) with the planned experiment boreholes (black, purple). (b) Layout cross-section of the borehole array. Six monitoring boreholes for tomographic surveys (BPF-1–6) are located above a central experiment borehole (BPF-7). (c) Photograph inside the casing of BPF-7 with a photogrammetric camera carriage showing some installations. (d) 3D model setup for numerical discontinuum simulations of the PF experiment. Note the global (XYZ) and local (xyz) coordinate systems.

3 PRELIMINARY RESULTS AND DISCUSSION

3.1 Pre-existing rock mass discontinuities and overbreaks

Analysis of optical images of all seven boreholes revealed tectonic faults of variable orientations. The great majority of these faults belong to one fault set with an average orientation of 139/43 ±11° (dip direction/dip angle and one standard deviation; Figure 2a,b), i.e., intersecting the central experimental borehole at an angle of on average 41° considering fault strike direction. These faults are of very similar orientation as the rock bedding (138/42). A second set of gently dipping fault planes oriented 108/18 ±13° is present, intersecting the experimental borehole at 34° on average considering the dip of the planes. In addition, a major fault zone known as the *main fault* was identified in all boreholes by its high content of scaly clay that led to small, structurally-controlled core surface and borehole wall breakouts. The fault zone thickness ranges between 0.49 m and 0.76 m and its mean thickness is 0.57 m (Bernasconi, 2020). The bounding fault planes of the fault zone (mean orientation: 135/47, borehole intersection angle: 45°) are slightly oblique to fault set 1 (compare red and yellow pole points to fault planes in Figure 2a,b). Finally, tectonic fault true spacing is greater SE (on average: 0.72 m) than NW (on average: 0.26 m) of the main fault zone.

Besides natural fractures, stress-induced borehole overbreaks formed during drilling and increased in size thereafter. Figure 2c shows the frontal section (2.5 m to 6 m) of the BPF-7 3D photogrammetric model from November 13th, 2020. A stress-induced borehole overbreak at the left side of the crown can be seen from the view looking toward West. Also, a gently dipping tectonic fault plane of the second fault set and the steeper, major tectonic fault zone are visible.

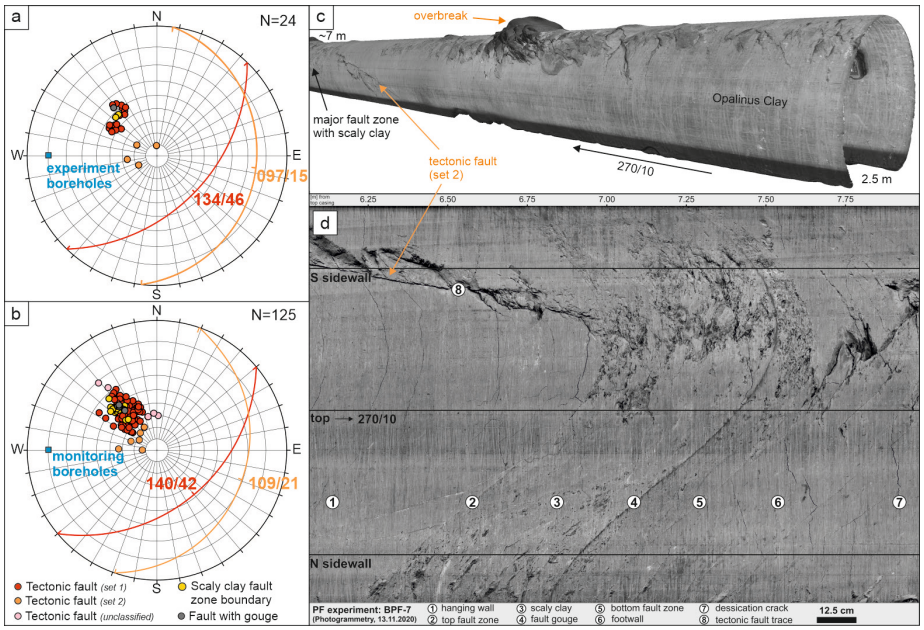

Figure 2. Pole points to fault planes (a) for BPF-7 and (b) for BPF-1–6. Equal angle, lower hemisphere projections. (c) Perspective view of the top part of the photogrammetric 3-D model of BPF-7 (Nov. 2020). (d) Rock mass structures around the major fault zone seen in an unwrapped 3-D model of BPF-7.

3.2 Electrical and seismic tomographies

Figure 3a shows a section of the baseline ERT model from 12/2020. One can detect higher resistivities in the frontal area up to 6.5 m. In the rear area from around 14 m, rather low resistivities dominate. Along BPF-1, there are some local high-resistive structures, which, however, are likely to represent numerical artefacts due to some electrode failure in this borehole. Compared to the baseline measurement, the repeat measurements of 03/2022 (Figure 3b) show a pronounced zone with lower resistivity in the areas of the main fault (purple planes) and adjacent footwall rock mass. One possible explanation is that rock mass dilatancy around the PF experiment borehole resulted in pathways for fluids, which is manifested by an increased electrical conductivity captured by the measurement. Note that wet spots were found in monitoring boreholes in the footwall rock mass.

Episodic seismic measurements show the anisotropic behaviour of the OPA (Figure 3c, top). Maximum p-wave velocities of 2965–3137 m/s were derived with an anisotropy factor of 17.5–21.1%. These values are in agreement with previous seismic measurements in the MT URL. Compared to the initial measurement of 9/2020 (blue), repeated measurements in 12/2020 (orange) and 11/2021 (green) show a decrease of the apparent velocities for the plane BPF1-BPF6, which is closest to the experiment borehole (Figure 1b). For opposite source and receiver locations (Figure 3c bottom), we observe a decrease of the apparent velocity around 9 m receiver depth in BPF6.

In Figure 3d, we show the monthly recordings for two exemplary, permanently-installed transmitter-receiver couples in boreholes BPF2-BPF5 (top) and BPF1-BPF-6 (bottom) from 04/2021 to 11/2021. While the first arriving waveforms remain very similar over the observation period, the later arriving coda waves show a gradual phase-shift that relates to an increase in seismic velocity. Besides the phase-shift, also an increase in amplitude can be observed.

3.3 Numerical simulation

Figure 4a illustrates the numerical simulation results of displacement distributions of rock mass (top) and faults (bottom) after the borehole drilling. For the displacement field of the rock mass, a conspicuous structurally-controlled pattern can be seen. For the displacement field of faults, noticeable displacements occur in the vicinity of the borehole. Figure 4b (top) shows the displacement and stress distributions of the rock mass at x = 8 m cross section. Locations with higher

fault frequency accommodate larger rock mass deformations. One can also note that the distribution of maximum principal stress is consistent with the expectation that the top left and bottom right corners of the borehole (looking down the hole from the top) display larger values of compressive stresses indicated by observations of borehole wall breakouts at these positions. Figure 4b (bottom) compares the overbreak patterns as observed in situ with those captured by the numerical simulation. Our numerical model captured many important features such as concentrated overbreaks at the top left corner of the borehole, which shows a good agreement with the experimental observation.

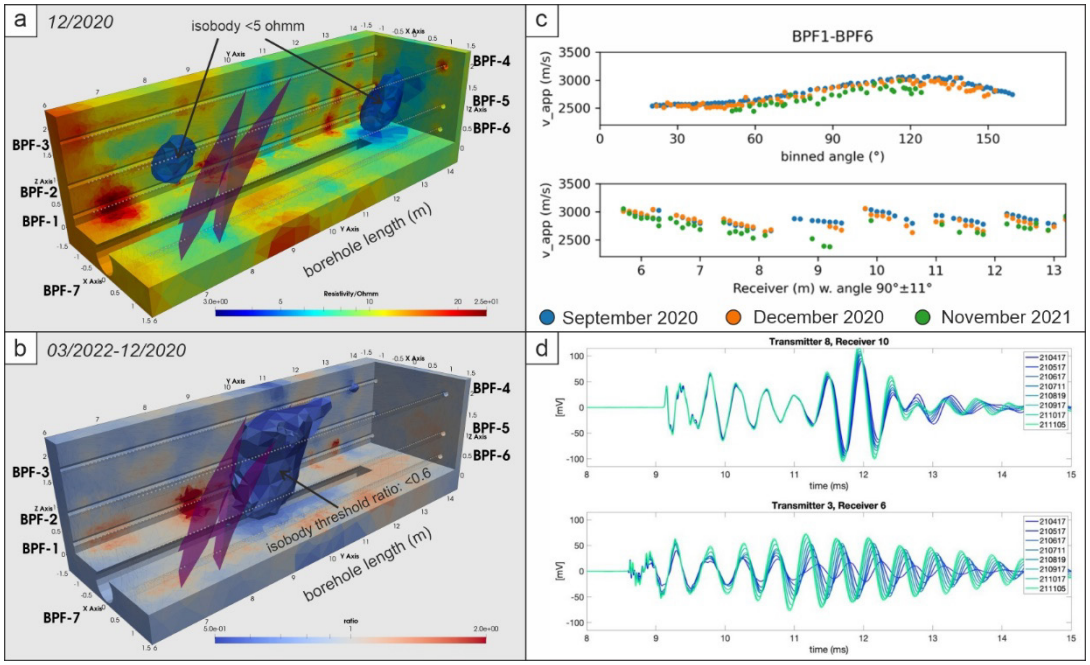

Figure 3. (a) Electrical resistivity of the rock mass between six monitoring boreholes at the depth range of 5.5–14.0 m from top of borehole casing from 12/2020. The colours indicate lower (blue) to higher (red) rock resistivities. The view shows cuts through the data model. (b) Relative changes between 12/2020 and 03/2022. Blue colours represent decreases and red colours increases in electrical resistivity. The purple planes describe the position of the main fault zone. (c) Apparent velocity for plane BPF1-BPF6 as of 9/2020 (blue), 12/2020 (orange), and 11/2021 (green), against source-receiver angle (top) and for opposite source and receiver positions (bottom). (d) Two exemplary transmitter receiver couples with monthly recordings from 04–11/2021. A phase shift and an amplitude change in the later arriving coda waves are apparent.

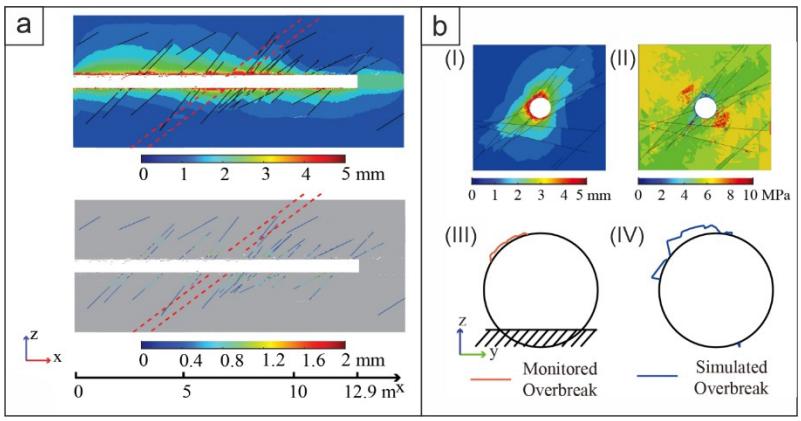

Figure 4. (a) Displacement distributions of rock mass (top) and faults (bottom) after borehole excavation. The red dashed lines indicate the location and thickness of the fault zone. (b) Borehole cross-sections at x = 8 m show (I) the distribution of rock mass displacements, (II) maximum principal stress magnitude, (III) monitored overbreak pattern (shadowed zone indicates a region that cannot be captured by the camera in the experiment borehole), and (IV) simulated overbreak pattern by the 3D numerical discontinuum model.

4 SUMMARY AND OUTLOOK

The PF experiment has been installed in 2020 and is since then ongoing. The rock mass discontinuities have been characterised in detail and used as an input for numerical discontinuum simulations. The in-situ data sets obtained over the last two years, together with the simulation results, are essential for investigating rock mass damage extents and identifying damage formation processes as well as assessing their spatial and temporal evolution. Regular photogrammetric surveys of the experiment borehole are used to assess the visible borehole failure evolution (Figure 2), while geophysical tomographic measurements explore changes of the rock mass in the crown of the experiment borehole (Figure 3). At present, not all obtained datasets have been processed and evaluated. First results indicate that for the relatively large intersection angles between experimental borehole direction and tectonic fractures (38–45°), only minor structurally-controlled breakouts occur during the ventilation phase. However, preliminary results by ERT highlight reduced electrical resistivity of a rock mass portion in the footwall of the major fault zone, which is as far as 2 m above the experiment borehole crown (Figure 3b), demonstrating a substantial radial extent of rock mass property changes that could originate from excavation-induced damage. In addition, repeat seismic measurements revealed changes in the near-field of the experimental borehole (Figure 3c,d) that may be relate to complex rock mass reactions during the ventilation period caused by rock mass convergence, desaturation, damage propagation and associated processes, which will be addressed in our future work. Finally, larger rock mass deformation magnitudes and extents were found in the footwall compared to the hanging wall by the numerical simulation (Figure 4a).

Over the next years, we will continue to monitor and interpret the in-situ rock mass behaviour. The final assessment of the results of the PF experiment will be based on an integration of multifold datasets to explore structurally-controlled failure evolution in the Opalinus Clay shale and its impact on HLW repository drifts.

ACKNOWLEDGEMENTS

The Swiss Federal Nuclear Safety Inspectorate (ENSI) and the Swiss Federal Office of Topography (swisstopo) are funding the PF experiment. We are also grateful to the Federal Institute for Geosciences and Natural Resources (BGR) in Germany for supporting the in-situ experiments with electrical resistivity and seismic surveys and analyses. Finally, the Swiss Seismological Service (SED) provided a data acquisition system and analysis of daily records of seismic data.

REFERENCES

Bernasconi, M. 2020. *Setup of photogrammetric borehole surveys and structural rock mass modelling of the Progressive Failure experiment (Mont Terri, Switzerland)*. M. Sc. thesis, Department of Earth Sciences, ETH Zurich.

Bieniawski, Z.T. 1989. *Engineering rock mass classifications*. New York: Wiley.

Birkholzer, J.T., Tsang, C.-F., Bond, A.E., Hudson, J.A., Jing, L., Stephansson, O. 2019. 25 years of DECOVALEX – Scientific advances and lessons learned from an international research collaboration in coupled subsurface processes, *Int. J. Rock Mech. Min. Sci.* 122, DOI: 10.1016/j.ijrmms.2019.03.015.

Zhao, C., Lei, Q., Ziegler, M., Loew, S. 2022. *3-D numerical simulation of structurally controlled, progressive failure of a large-diameter experiment borehole*. Extended abstract and oral presentation. 2nd Progressive Rock Failure Conference, Flat Rock, NC, USA, 20–24 June.

Ziegler, M., Loew, S. 2020. Mont Terri PF experiment: Progressive failure of structurally-controlled overbreaks — Project introduction and overview of work program, *ENSI Erfahrungs- und Forschungsbericht* 2019, 307–315.

Ziegler, M., Loew, S. 2021a. Mont Terri PF experiment: Progressive failure of structurally-controlled overbreaks — Site characterisation and in-situ experiment installations. *ENSI Erfahrungs- und Forschungsbericht* 2020, 291–299.

Ziegler, M., Loew, S. 2021b. PF-Experiment: Installation and first data. *Mont Terri Technical Note* 2020–37.